Full Paper

Journal of the Brazilian Chemical Society

https://dx.doi.org/10.21577/0103-5053.20260074

J. Braz. Chem. Soc. **2026**, *37-Spe2*, e-20260074, 1-14

α-Nitroolefins as Dipolarophiles for the Synthesis of 1,4-Disubstituted 1,2,3-Triazoles

Meire Y. Kawamura[a] *and Marco Antonio B. Ferreira*[*,a]

[a]*Departamento de Química, Universidade Federal de São Carlos (UFSCar), 13565-905 São Carlos-SP, Brazil*

α-Nitroolefins are introduced as novel dipolarophiles in [3 + 2] cycloadditions with organic azides, enabling the regioselective synthesis of 1,4-disubstituted 1,2,3-triazoles under metal-free conditions. The α-nitroolefin is generated *in situ* from the corresponding nitro alcohol-derived acetate. Reaction optimization identified Brønsted acid catalysis in dimethylformamide (DMF) under microwave irradiation as the optimal conditions, affording triazoles in yields up to 71%. The methodology tolerates a range of aryl-substituted α-nitroolefins and aliphatic azides, although aryl azides exhibit diminished reactivity. Computational studies reveal that the cycloaddition proceeds preferentially through a stepwise mechanism. Regioselectivity arises from a combination of favorable frontier molecular orbital interactions and a lower-distortion energy pathway, in which azide deformation plays a dominant role. These findings provide a mechanistic basis for the exclusive formation of 1,4-triazoles and highlight the impact of nitro group positioning on cycloaddition reactivity.

Keywords: α-nitroolefins, 1,3-dipolar cycloaddition, triazoles, distortion-interaction analysis, DFT

Introduction

1,2,3-Triazoles occupy a privileged position among synthetic nitrogen-containing heterocycles due to their remarkable thermal and hydrolytic stability, rigid π-conjugated framework, and broad relevance in medicinal chemistry, chemical biology, and materials science.[1-6] Their synthetic prominence is closely associated with the development of 1,3-dipolar cycloaddition chemistry, especially the classical Huisgen cycloaddition between azides and alkynes, which established a general platform for triazole construction.[7,8] A major advance came with the independent development of the copper(I)-catalyzed azide-alkyne cycloaddition (CuAAC) by the Sharpless/Fokin and Meldal groups, providing a highly efficient and regioselective route to 1,4-disubstituted 1,2,3-triazoles under mild conditions.[3,9-12] In a complementary manner, ruthenium catalysis enabled selective access to the corresponding 1,5-disubstituted regioisomers.[13] Even so, the search for alternative triazole-forming strategies remains highly attractive, particularly related to metal-free processes and complementary dipolarophiles.

In this broader context, metal-free triazole chemistry has expanded far beyond the original thermal azide-alkyne paradigm. In addition to strain-promoted azide-alkyne cycloaddition, which offers a bioorthogonal solution that avoids cytotoxic transition metals, a variety of organocatalytic and metal-free methods based on electronically activated unsaturated systems have emerged as conceptually distinct alternatives for triazole synthesis. Enamines, enolates, iminium ions, vinyl sulfones, and related activated alkenes can act as competent dipolarophiles in azide [3 + 2] cycloadditions (Scheme 1a), opening access to 1,2,3-triazoles through reaction manifolds that differ substantially from classical CuAAC chemistry.[14-22] These developments are especially relevant because they not only broaden the synthetic scope of azide cycloadditions, but also raise important mechanistic questions concerning substrate activation, cycloaddition topology, elimination/aromatization steps, and the origins of regioselectivity.

Among electronically activated alkenes, nitroolefins occupy a particularly attractive position as 1,3-dipolarophiles. β-Nitroolefins are readily accessible, strongly polarized alkenes that can undergo [3 + 2] cycloaddition with azides followed by elimination of HNO_2 to furnish aromatic 1,2,3-triazoles (Scheme 1a, equation 3).[14,23-27] Seminal studies showed that β-nitroolefins react with sodium azide or trimethylsilyl azide to provide *NH*-1,2,3-triazoles, thereby

*e-mail: marco.ferreira@ufscar.br
Editor handled this article: Giovanni Wilson Amarante (Executive)
This publication is part of the special issue "Organic Synthesis - BMOS"

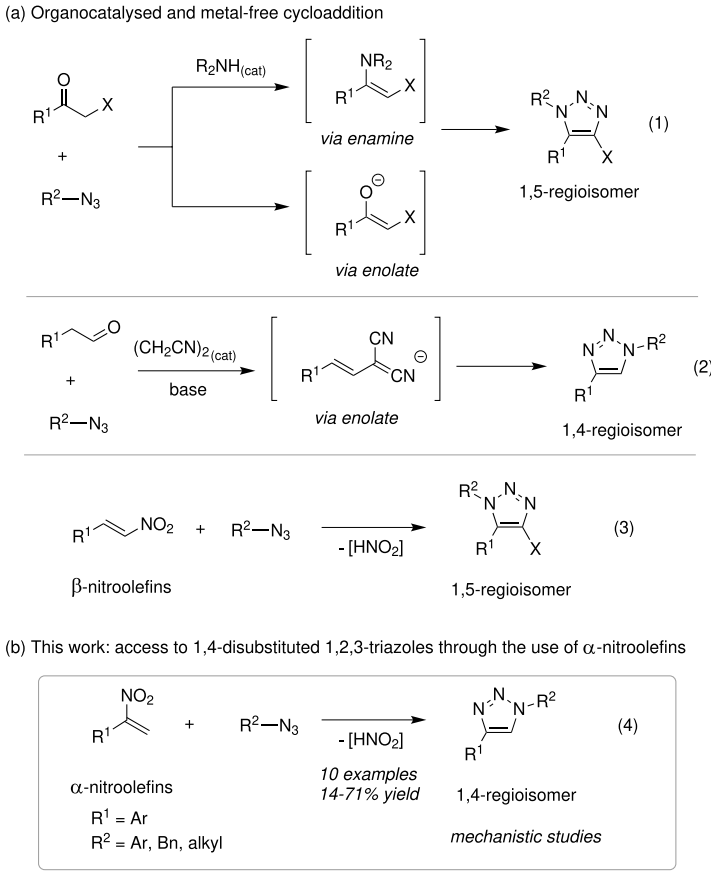

Scheme 1. (a) Emerging approaches to 1,2,3-triazoles via 1,3-dopolar cycloaddition. (b) [3 + 2] Cycloadditions involving α-nitroolefins and organic azides to produce 1,4-dissubstituted 1,2,3-triazoles.

defining β-nitroolefins as viable dipolarophiles for triazole synthesis.[23-26] Subsequent reports further demonstrated that cycloadditions of organic azides with β-nitroolefins can also furnish *N*-substituted triazoles, although early catalyst-free protocols often proceeded with modest yields and long reaction times.[14,27] In contrast, organocatalytic, Brønsted acid-mediated, and metal-catalyzed variants significantly improved chemical yields and regioselectivities, while multicomponent approaches involving *in situ* β-nitroolefin generation further expanded the synthetic scope of this chemistry.[28-31] Other dipoles have also been explored in 1,3-dipolar cycloadditions, enabling access to heterocycles such as cyanopyrazoles, isoxazoles, and pyrazolo[1,5-*c*] quinazolines.[32-34] These studies established β-nitroolefins as a distinctive and synthetically valuable class of dipolarophiles in the search for more efficient and regioselective triazole syntheses.

At the same time, β-nitroolefin cycloadditions remain mechanistically much less understood than their alkyne-based counterparts. Particularly, mechanistic investigations of azide cycloadditions involving activated alkenes remain scarce. In a recent study, we showed that reactions of β-nitroolefins proceed through a rate-determining cycloaddition step involving an asynchronous transition structure and showing a strong kinetic preference for the 1,5-regioisomer.[18] Distortion/interaction-activation strain and energy decomposition analyses further indicated that this preference arises from a favorable balance of distortion, electrostatic, and dispersion interactions in the transition state leading to the major cycloadduct.

On this basis, we questioned whether changing the position of the nitro group along the olefinic framework could redirect the regiochemical outcome of the reaction, providing access to 1,4-regioisomer while preserving the main synthetic advantages already associated with nitroolefins (Scheme 1b). In this context, the α-nitroolefins, a previously unexplored structural pattern in azide [3 + 2] cycloadditions, emerged as especially promising substrates. From a physical-organic perspective, relocating the nitro group from the β- to the α-position should significantly alter alkene polarization, azide approach geometry, and the steric/electronic balance in the regioselectivity-determining transition structures.

Herein, we report that α-nitroolefins act as new dipolarophiles for a highly regioselective access to the 1,4-disubstituted 1,2,3-triazoles from organic azides.

Theoretical studies further indicate that this regiodivergent outcome arises from the combined action of electronic and steric effects in the key transition structures, including more favorable frontier orbital interactions and a preferred arrangement in which the bulkier substituents remain spatially opposed. This study advances the mechanistic understanding of eliminative azide-olefin cycloadditions and clarifies how subtle structural changes in nitroolefin architecture can control regiochemical divergence in triazole synthesis.

Results and Discussion

Reaction optimization

The preparation of the α-nitroolefin intermediate started from the corresponding nitroalcohol **2** was initially investigated using several dehydration strategies. Based on this strategy, the preparation of the required nitro-arylbenzene **1a-1d** was initially carried out (Scheme 2). Thus, nucleophilic substitution between organo halide compounds and nitrite afforded **1a-1d**.[35] Subsequently, following a Henry-type approach, reaction of nitro compound with *p*-formaldehyde under basic conditions and heating provided 2-nitro-2-arylethanol **2a-2d**.[36]

Initial attempts toward the preparation of the α-nitroolefin from the corresponding nitroalcohol **2a** under classical dehydration conditions proved unsuccessful.[37] Treatment with phthalic anhydride, either under solvent-free conditions or in toluene, led to complex mixtures, likely due to substrate decomposition at elevated temperatures (Table S1, Supplementary Information (SI) section). Alternatively, mesylation conditions ($MsCl/Et_3N$) enabled the formation of the desired α-nitroolefin in low yield, but increasing the temperature or base loading resulted predominantly in isomerization to the corresponding β-nitrostyrene (Table S1, entries 3-5). This behavior is consistent with base-promoted isomerization pathways reported in the literature.[38]

Given these limitations, we turned our attention to an alternative strategy involving the *in situ* generation of the α-nitroolefin **3**. To this end, the corresponding acetate derivative **4** was prepared from the nitroalcohol precursor **2**, enabling elimination under acidic conditions and avoiding basic media (Scheme 3).

The [3 + 2] cycloaddition between the *in situ* generated α-nitroolefin and benzyl azide was then investigated (Table 1). Initial conditions using morpholine/*p*-toluenesulfonic acid (PTSA) resulted exclusively in isomerization of the intermediate to β-nitroolefin (entry 1).[30] Brønsted acid conditions were evaluated using PTSA as catalyst,[28] and a systematic variation of solvent, concentration, and temperature revealed a strong dependence of the reaction outcome on these parameters (Table 1, entries 2-7). Reactions performed in dimethyl sulfoxide (DMSO) provided either trace amounts or modest yields of the desired product (entries 2-3), whereas switching to dimethylformamide (DMF) significantly improved the efficiency of the process (entries 4-7). Increasing the reaction concentration proved beneficial, with the optimal result obtained at 0.75 M, affording the desired triazole in 68% yield (entry 6). A further increase in concentration led to a slight decrease in yield (entry 7).

The effect of catalyst loading, azide stoichiometry, and solvent was further examined. Reducing the PTSA loading from 50 to 25 mol% resulted in essentially unchanged yield of 66% (Table 1, entry 8), while the reaction still proceeded in the absence of catalyst, albeit with diminished efficiency (49%, entry 9). Increasing the amount of benzyl azide did not significantly affect the outcome (entry 10). Solvent screening confirmed DMF as the optimal medium, as alternative solvents such as DMSO, acetonitrile, and PEG400 resulted in lower yields or only trace product formation (entries 11-13). Microwave-assisted conditions were next evaluated as an alternative to conventional heating (entry 14-15). Under otherwise identical conditions, a significant reduction in reaction time was observed (from 16 h to 1 h 20 min), with only a slight decrease in yield (entry 14). Increasing

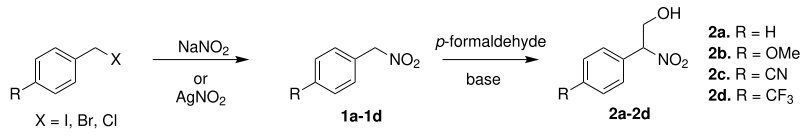

Scheme 2. General strategy for the synthesis of **1a-1d** and **2a-2d** compounds.

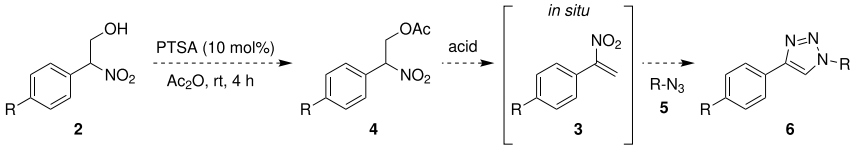

Scheme 3. Synthetic strategy for the *in situ* generation of the α-nitroolefin under [3 + 2] cycloaddition conditions.

Table 1. Conditions evaluated for the [3 + 2] cycloaddition between α-nitroolefin **3a** and benzyl azide **5a**[a]

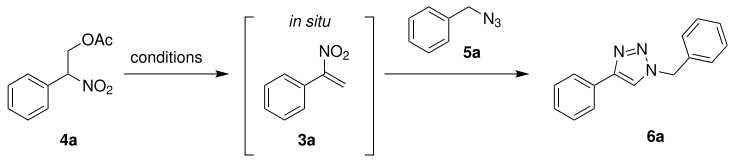

entry No.	Catalyst (concentration / mol%)	Solvent	Concentration / M	Temperature / °C	time / h	Yield (**6a**)[b] / %
1	Morph/PTSA (50)	DMSO	1.5	50	3	isomerization
2	PTSA (50)	DMSO	0.3	40-70	72	< 5
3	PTSA (50)	DMSO	0.1	100	4	23
4	PTSA (50)	DMF	0.1	110	23	38
5	PTSA (50)	DMF	0.5	110	16	51
6	PTSA (50)	DMF	0.75	110	16	68
7	PTSA (50)	DMF	1.0	110	16	63
8	PTSA (25)	DMF	0.75	110	16	66
9	–	DMF	0.75	110	16	49
10[c]	PTSA (25)	DMF	0.75	110	16	69
11	PTSA (25)	DMSO	0.75	110	16	34
12	PTSA (25)	MeCN	0.75	110	16	< 5
13	PTSA (25)	PEG400	0.75	110	16	< 5
14[d]	PTSA (25)	DMF	0.75	110	1 h 20 min	66
15[d]	PTSA (25)	DMF	0.75	130	50 min	71

[a]General condition: **4a** (0.24 mmol, 1.0 equiv.), **5a** (1.1 equiv.), and catalyst in anhydrous solvent (0.1-1.5 M) were stirred at the indicated temperature and time, under either conventional heating or microwave irradiation. [b]Isolated yield after column chromatography in silica flash. [c] **5a** (1.5 equiv.). [d]Microwave irradiation (300 W). DMSO: dimethyl sulfoxide; DMF: dimethylformamide; PTSA: *p*-toluenesulfonic acid.

the temperature to 130 °C led to improved efficiency, affording the product in 71% yield within 50 min (entry 15), representing the optimal conditions identified in this study. Other solvents such as toluene and ethyl acetate proved ineffective under microwave irradiation.

Substrate scope and limitations

The substrate scope of the reaction was then investigated (Scheme 4). With respect to the α-nitroolefin component, aryl-substituted substrates bearing both electron-donating and electron-withdrawing groups were evaluated. The *p*-methoxy-substituted substrate afforded 1,4-disubstituted 1,2,3-triazole **6b** in 44% yield, while electron-deficient derivatives containing cyano and trifluoromethyl groups provided the corresponding products **6c** and **6d** in 41 and 31% yields, respectively. Overall, these results indicate that electronic variations on the aryl ring are tolerated, although only moderate to low yields were obtained. This behavior highlights a limitation of the present system, as changes in the electronic nature of the α-nitroolefin do not translate into significant improvements in reaction efficiency.

The scope with respect to the azide component revealed a stronger dependence on substrate structure (Scheme 3). Aliphatic azides proved to be more suitable reaction partners, providing improved yields in the case of cyclopentyl (**6e**, 69%), dodecyl (**6f**, 55%), and carboethoxymethyl substrates (**6g**, 60%). In contrast, no product formation was observed for the benzoylmethyl group (**6h**), likely due to substrate instability under the acidic and high temperature reaction conditions. Aryl azides were also evaluated resulting in diminished yields. Phenyl azide afforded product **6i** in 45% yield, while the *p*-methoxy-substituted analogue **6j** was obtained in only 14% yield. These lower yields are attributed to the known instability of aryl azides under acidic and high-temperature conditions, as well as to a poorer electronic demand match with the electron-deficient nitroolefin. Taken together, these results indicate that substrate stability and electronic demand matching are key factors governing the efficiency of this transformation.

The exclusive formation of the 1,4-regioisomer was observed across the substrate scope, with no detection of the corresponding 1,5-isomer. This behavior highlights the inherent regioselectivity of the present system. In contrast

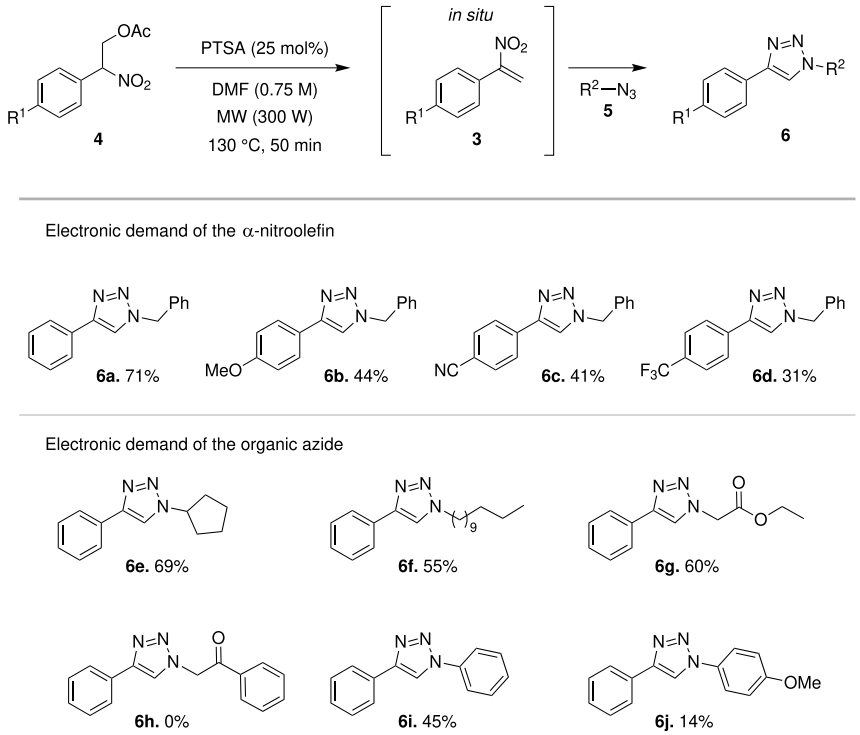

Scheme 4. Substrate scope for the [3 + 2] cycloaddition between α-nitroolefins **3** and organic azides **5**.

to classical CuAAC reactions, which rely on terminal alkynes under transition-metal catalysis, the present system operates through electronically activated α-nitroolefins as dipolarophiles under metal-free conditions. Additionally, in contrast to related protocols (Scheme 1a, equation 2),[16] which require basic conditions for the generation of the reactive dipolarophile, the present system operates under acidic conditions, enabling *in situ* formation of the α-nitroolefin and subsequent cycloaddition in a single step. Notably, this reactivity is also distinct from that of β-nitroolefins, which typically lead to complementary regioselectivity patterns. Together, these results demonstrate that α-nitroolefins provide a complementary and regiodivergent platform for triazole synthesis.

Theoretical mechanistic studies

Our next step was to perform computational studies on the reaction between the α-nitroolefin and organic azides in order to gain mechanistic insight into this new cycloaddition manifold leading to 1,4-disubstituted triazoles. To this end, the possible reaction pathways leading to both the 1,4- and 1,5-disubstituted 1,2,3-triazole regioisomers were investigated using the α-nitroolefin **3a** and two representative organic azides, namely BnN_3 (**5a**), and PhN_3 (**5g**) (Scheme 5). Based on our previous studies on the reactions of β-nitroolefins with organic and inorganic azides,[18] in which the elimination step was found not to be selectivity-determining, we focused our analysis on the cycloaddition stage of the reaction and did not investigate the subsequent HNO_2 elimination step for the α-nitroolefin system.

A general inspection of the computed free-energy profiles for the cycloaddition step (Schemes 6a-6b) indicates that, regardless of the azide employed, the lowest-energy pathway leads to formation of the 1,4-triazole and occurs preferentially through a stepwise mechanism rather than through a concerted process.

For the pathway leading to the 1,4-triazole (Scheme 6a), we were unable to locate a concerted transition state (**TS-1**) for the reaction with BnN_3 (**5a**), despite extensive exploration of the potential energy surface using different initial guesses and computational strategies. This inability to identify **TS-1** does not exclude the possibility of a concerted pathway. In contrast, the stepwise pathway **TS-2** could be fully characterized. Comparison between the transition states associated with azide attack (**TS-2**, relative Gibbs free energies ($\Delta G^{\ddagger}$) = 31.8 kcal mol^{-1}) and ring closure (**TS-3**, $\Delta G^{\ddagger}$ = 33.5 kcal mol^{-1}) indicates that, although **TS-3** lies slightly higher in energy relative to the reactants, the ring-closing step occurs with a very small barrier (3 kcal mol^{-1}) from the intermediate **I-2** and is therefore expected to be extremely fast.

For PhN_3 (**5g**) (Scheme 6b), a different scenario emerges. In this case, both a concerted pathway (**TS-1**, $\Delta G^{\ddagger}$ = 36.0 kcal mol^{-1}) and a stepwise (**TS-2**, $\Delta G^{\ddagger}$ = 35.2 kcal mol^{-1}) transition states were located, with a

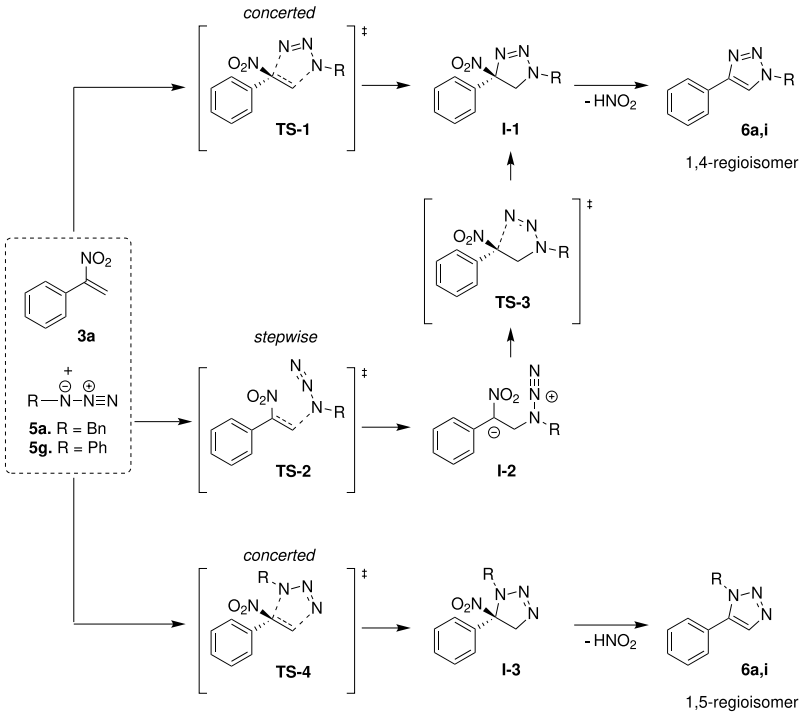

Scheme 5. Computed reaction pathways for the cycloaddition of α-nitroolefin **3a** with BnN_3 (**5a**), and PhN_3 (**5g**), leading to the 1,4- and 1,5-triazole regioisomers.

small energy difference of 0.7 kcal mol^{-1}, indicating a near-degeneracy between these two mechanistic possibilities. However, no ring-closing transition state (**TS-3**) could be located for PhN_3, suggesting again that the corresponding intermediate **I-2** collapses rapidly to **I-1**. Additionally, the energy barriers calculated for PhN_3 (**5g**) are consistent with the lower experimental efficiency observed for aryl azides. The activation barrier for **TS-2** increases by 3.4 kcal mol^{-1} relative to BnN_3 (**5a**), reflecting a less favorable cycloaddition that can be attributed to the lower electron density of aryl azides.

From a regioselectivity standpoint, the preference for formation of the 1,4-triazole can be rationalized based on both electronic and steric factors. Consistent with frontier molecular orbital (FMO) considerations, the favored pathway involves interaction between the terminal nitrogen of the azide and the methylene carbon of the α-nitroolefin, which displays the largest highest occupied molecular orbital (HOMO)-lowest unoccupied molecular orbital (LUMO) coefficients, leading to a more favorable orbital overlap in the corresponding transition state (Scheme 7a). In addition to these orbital effects, distortion-interaction analysis provides further insight into the origin of the preference for the stepwise **TS-2** over the concerted **TS-1** and **TS-4** (Scheme 7b).[19] Although **TS-1** benefits from a larger interaction energy due to the simultaneous formation of two bonds, it is significantly penalized by a higher distortion energy, especially associated with deformation of the azide fragment. In particular, the azide undergoes substantial bending energy distortion ($\Delta E_d^{\ddagger}$) in **TS-1** ($\angle_{N-N-N} = 142°$, $\Delta E_{d,azide}^{\ddagger} = 18.0$ kcal mol^{-1}), whereas it remains much closer to linearity in **TS-2** ($\angle_{N-N-N} = 173.7°$, $\Delta E_{d,azide}^{\ddagger} = 2.7$ kcal mol^{-1}), resulting in a noticeably lower-distortion energy for the latter. This trend is quantitatively supported by the total distortion energy ($\Delta E_{d,total}^{\ddagger}$). **TS-2** showing a significantly lower total distortion energy (24.3 kcal mol^{-1}) compared to **TS-1** (29.73 kcal mol^{-1}). The higher energy of **TS-4** can also be understood within this basis, requiring further distortion of the azide ($\angle_{N-N-N} = 137.8°$, $\Delta E_{d,azide}^{\ddagger} = 25.6$ kcal mol^{-1}), leading to a substantial increase in distortion energy. Finally, the balance between distortion and interaction favors the stepwise **TS-2** despite its less favorable interaction energy ($\Delta E_i^{\ddagger}$), highlighting the dominant role of azide deformation in controlling the relative energetics of the competing transition states.[19] These results are in line with previous observations reported for related β-nitroolefin systems.[18]

Conclusions

In summary, we have demonstrated that α-nitroolefins act as effective dipolarophiles in metal-free [3 + 2] cycloadditions with organic azides, enabling regioselective access to 1,4-disubstituted 1,2,3-triazoles. The use of an *in situ* generation strategy proved essential to overcome the intrinsic instability and isomerization tendencies

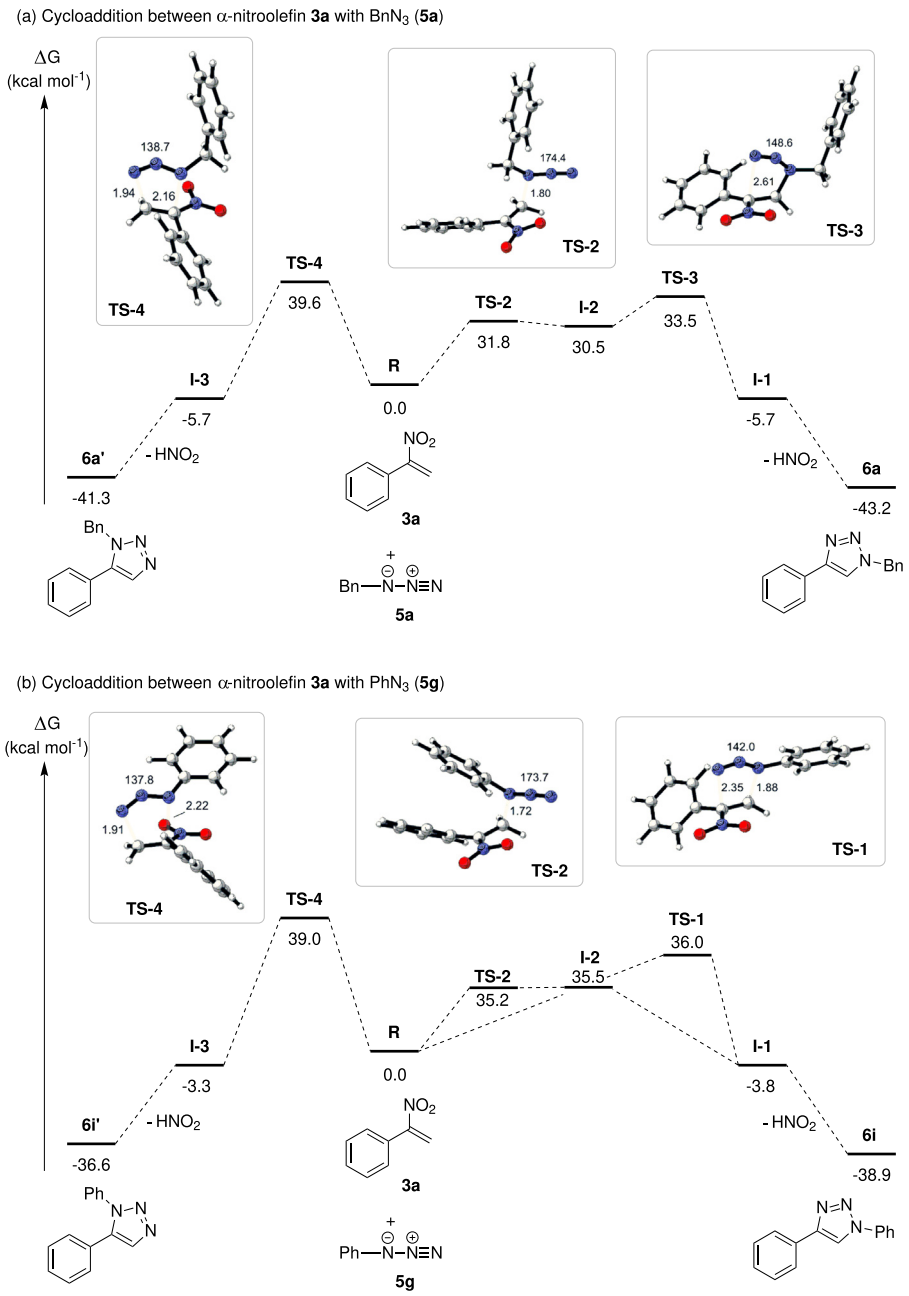

Scheme 6. Relative Gibbs free energies (kcal mol^{-1}) calculated for the cycloaddition between α-nitroolefin **3a** with BnN_3 (**5a**), and PhN_3 (**5g**), at the M06-2X/def2-TZVP level (Integral Equation Formulation of Polarizable Continuum Model (IEF-PCM), DMF).

of α-nitroolefins under basic conditions, allowing their productive engagement in cycloaddition chemistry.

The reaction displays complete regioselectivity across the explored substrate scope, with a clear dependence on the nature of the azide, particularly highlighting the superior performance of aliphatic over aryl azides. These trends were rationalized through computational studies, which indicate that the cycloaddition step is both rate- and selectivity-determining and proceeds preferentially via a stepwise mechanism.

Detailed mechanistic analysis revealed that regioselectivity originates from a combination of electronic and steric effects. Favorable frontier molecular orbital interactions promote the approach leading to the 1,4-regioisomer, while distortion-interaction analysis shows that reduced azide distortion is the dominant factor lowering the activation barrier for the preferred pathway. In contrast, competing pathways are penalized by increased geometric distortion, particularly in the azide fragment.

Overall, this study establishes α-nitroolefins as a new class of dipolarophiles for triazole synthesis and provides fundamental insights into how subtle structural

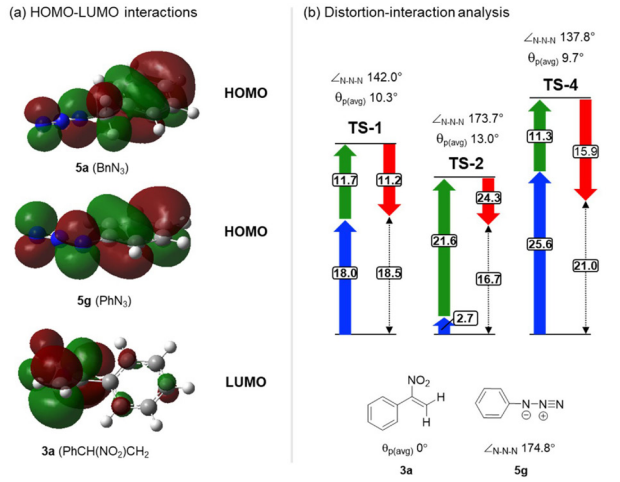

Scheme 7. (a) Frontier molecular orbital (FMO) analysis illustrating the electronic demand match between the azide and the α-nitroolefin, favoring formation of the 1,4-triazole. (b) Distortion-interaction analysis of the competing transition states, showing the contributions of distortion ($\Delta E_d^{\ddagger}$) and interaction ($\Delta E_i^{\ddagger}$) energies to the overall activation barrier. M06-2X/def2-TZVP level (IEF-PCM, DMF) (black lines, activation energies $\Delta E^{\ddagger}$; blue, distortion energies $\Delta E_{d,azide}^{\ddagger}$ of **5g**; green, distortion energies $\Delta E_{d,\alpha\text{-nitrostyrene}}^{\ddagger}$ of **3a**; red, interaction energies $\Delta E_i^{\ddagger}$). Energies in kcal mol^{-1}.

modifications in nitroolefins can control reactivity and regioselectivity in azide cycloadditions.

Experimental

All reagents and solvents were purchased from commercial sources (Merck, Sigma-Aldrich) and were used as received. Solvents were dried using standards technics. Analytical thin layer chromatography (TLC) was performed using 250 μm silica gel Merck DC Kieselgel 60 (230-400 mesh) pre-coated plates and performed using UV light. Flash column chromatography was performed using 60 Å, 70-230 mesh Aldrich Co silica gel. Microwave reactions were performed in sealed tubes using a self-tuning CEM Discover® focused monomode microwave synthesizer, with temperature monitored in real time by the built-in infrared sensor. Reactions were conducted at the specified temperatures under a fixed power of 300 W. ^{1}H and ^{13}C nuclear magnetic resonance (NMR) spectra were measured in $CDCl_3$ using a Bruker Advance 400 (9.4 Tesla). Chemical shifts are reported relative to tetramethylsilane (TMS) reported in ppm. High resolution mass spectra (HRMS) were obtained using a Waters Acquity UPLC H-Class coupled with a Waters Xevo G2-XS QToF mass spectrometer equipped with an electrospray ionization (ESI) interface.

General procedure I for nitration

Nitromethylbenzene (**1a**)

Sodium nitrite ($NaNO_2$) (1.2 g, 17.5 mmol, 1.5 equiv.) and DMF (11.7 mL) were combined, and urea (1.4 g, 23.4 mmol, 2.0 equiv.) was added. The mixture was stirred at room temperature until complete dissolution of urea. The resulting solution was cooled to −10 °C, and a solution of benzyl bromide (2.0 g, 11.7 mmol, 1.0 equiv.) in DMF (11.7 mL) was added dropwise via an addition funnel. The reaction mixture was maintained at −10 °C under stirring for 6 h. Upon completion, ice-cold water (120 mL) was added, and the mixture was extracted with cold diethyl ether (3 × 60 mL). The combined organic layers were washed with saturated aqueous NaCl, dried over anhydrous Na_2SO_4, filtered, and concentrated under reduced pressure. Purification by flash column chromatography (5% EtOAc/hexanes) afforded nitromethylbenzene (**1a**) (770 mg, 5.6 mmol, 48%) as a pale-yellow oil. Spectroscopic data for this compound is in accordance with the literature.[39] Rf = 0.43 (10% EtOAc/hexanes); ^{1}H NMR (400 MHz, $CDCl_3$) δ 7.49-7.39 (m, 5H), 5.44 (s, 2H); ^{13}C NMR (101 MHz, $CDCl_3$) δ 130.1, 129.8, 129.2, 80.1.

p-Methoxy nitromethylbenzene (**1b**)

Prepared according to general procedure I. Purification by flash column chromatography on silica gel (5-10% EtOAc/hexanes gradient) afforded the product (3.36 g, 20.1 mmol, 24%) as a yellow oil. Rf = 0.34 (10% EtOAc/hexanes). Spectroscopic data for this compound is in accordance with the literature.[40] ^{1}H NMR (400 MHz, $CDCl_3$) δ 7.37 (d, *J* 8.4 Hz, 2H), 6.93 (d, *J* 8.5 Hz, 2H), 5.36 (s, 2H), 3.82 (s, 3H).

General procedure II for nitration

p-Cyano nitromethylbenzene (**1c**)

A solution of NaI (0.449 g, 3.0 mmol, 2.0 equiv.) in anhydrous acetone (2.6 mL) was added to a solution of *p*-cyanobenzyl bromide (0.294 g, 1.50 mmol, 1.0 equiv.) in anhydrous acetone (3.9 mL) at room temperature under stirring. The reaction mixture was stirred for 1 h, then filtered through Celite using acetone. The solvent was removed under reduced pressure, and the residue was dissolved in dichloromethane and filtered through Celite again. The organic phase was washed with saturated aqueous $Na_2S_2O_3$ and water, dried over anhydrous Na_2SO_4, filtered, and concentrated under reduced pressure to afford *p*-cyanobenzyl iodide as a yellow solid. The obtained solid (0.317 g) was dissolved in diethyl ether (13 mL) and added dropwise to a suspension of silver nitrite ($AgNO_2$) (0.300 g, 1.95 mmol, 1.5 equiv.) in diethyl ether (3.25 mL) at 0 °C under stirring (flask protected from light with aluminum foil). The reaction mixture was stirred overnight in an ice bath. The mixture was then filtered through Celite using

diethyl ether, dried over anhydrous $MgSO_4$, filtered, and concentrated under reduced pressure to afford nitromethyl *p*-cyanobenzene (**1c**) (42 mg, 0.26 mmol, 17% over two steps) as a pale-yellow solid. Spectroscopic data for this compound is in accordance with the literature.[40] Rf = 0.14 (10% EtOAc/hexanes, twice eluted); ^{1}H NMR (400 MHz, $CDCl_3$) δ 7.75 (d, *J* 8.0 Hz, 2H), 7.60 (d, *J* 8.0 Hz, 2H), 5.51 (s, 2H); ^{13}C NMR (101 MHz, $CDCl_3$) δ 134.0, 132.8, 130.7, 117.8, 114.1, 79.0.

p-(Trifluoromethyl)nitromethylbenzene (**1d**)

Prepared according to general procedure II. The product was obtained as a yellow oil (108 mg, 0.53 mmol, 56% over two steps). Spectroscopic data for this compound is in accordance with the literature.[39] Rf = 0.57 (20% EtOAc/hexanes); ^{1}H NMR (400 MHz, $CDCl_3$) δ 7.71 (d, *J* 8.0 Hz, 2H), 7.60 (d, *J* 8.0 Hz, 2H), 5.50 (s, 2H).

General procedure III for Henry reaction

2-Nitro-2-phenylethanol (**2a**)

A solution of **1a** (1.7 g, 12.7 mmol, 1.0 equiv.) in THF (141 mL) was treated with NaOAc (1.4 g, 12.7 mmol, 1.0 equiv.) and *p*-formaldehyde (380 mg, 12.7 mmol, 1.0 equiv.). The resulting mixture was heated at 50 °C and stirred for 3 h. Upon completion, the reaction mixture was filtered, and the solvent was removed under reduced pressure. Purification by flash column chromatography on silica gel (25% EtOAc/hexanes) afforded **2a** (1.8 g, 10.8 mmol, 84%) as a white solid. Spectroscopic data for this compound is in accordance with the literature.[36] Rf = 0.34 (25% EtOAc/hexanes); ^{1}H NMR (400 MHz, $CDCl_3$) δ 7.54-7.35 (m, 5H), 5.63 (dd, *J* 9.8, 3.7 Hz, 1H), 4.59 (dd, *J* 12.6, 9.8 Hz, 1H), 3.97 (dd, *J* 12.6, 3.7 Hz, 1H), 2.25 (s, 1H); ^{13}C NMR (101 MHz, $CDCl_3$) δ 131.5, 130.3, 129.3, 127.7, 92.3, 63.9.

2-Nitro-2-(*p*-methoxyphenyl)ethanol (**2b**)

Prepared according to the general procedure III. The product was obtained as a yellow oil (418 mg, 2.12 mmol, 71%). Rf = 0.14 (20% EtOAc/hexanes); ^{1}H NMR (400 MHz, $CDCl_3$) δ 7.35 (d, *J* 8.6 Hz, 2H), 6.92 (d, *J* 8.6 Hz, 2H), 5.57 (dd, *J* 9.8, 3.7 Hz, 1H), 4.57 (dd, *J* 12.5, 10.0 Hz, 1H), 3.94 (dd, *J* 12.5, 3.7 Hz, 1H), 3.81 (s, 3H), 2.29 (s, 1H); ^{13}C NMR (101 MHz, $CDCl_3$) δ 160.9, 129.1, 123.5, 114.5, 91.7, 63.7, 55.3; HRMS (ESI) *m/z*, calcd. for $[C_9H_{11}NO_4 + Na]^+$: 220.0586, found: 220.0580.

2-Nitro-2-(*p*-cyanophenyl)ethanol (**2c**)

Prepared according to the general procedure III. The product was obtained as a colorless oil (85.2 mg, 0.44 mmol, 64%). Rf = 0.29 (40% EtOAc/hexanes); ^{1}H NMR (400 MHz, $CDCl_3$) δ 7.74 (d, *J* 8.1 Hz, 2H), 7.56 (d, *J* 8.1 Hz, 2H), 5.67 (dd, *J* 9.1, 3.6 Hz, 1H), 4.58-4.49 (m, 1H), 4.08-3.99 (m, 1H), 2.39 (t, *J* 5.7 Hz, 1H); ^{13}C NMR (101 MHz, $CDCl_3$) δ 135.9, 132.9, 128.6, 117.7, 114.3, 91.2, 63.5; HRMS (ESI) *m/z*, calcd. for $[C_9H_8N_2O_3 + H]^+$: 193.0608, found: 193.0601.

2-Nitro-2-(*p*-trifluoromethylphenyl)ethanol (**2d**)

Prepared according to the general procedure III. The product was obtained as a colorless oil (42.5 mg, 0.18 mmol, 41%). Spectroscopic data for this compound is in accordance with the literature.[36] Rf = 0.26 (20% EtOAc/hexanes); ^{1}H NMR (400 MHz, $CDCl_3$) δ 7.69 (d, *J* 8.1 Hz, 2H), 7.56 (d, *J* 8.1 Hz, 2H), 5.70 (dd, *J* 9.5, 3.6 Hz, 1H), 4.61-4.50 (m, 1H), 4.06-3.94 (m, 1H), 2.85 (s, 1H); ^{13}C NMR (101 MHz, $CDCl_3$) δ 134.9, 132.4 (q, *J* 32.9 Hz), 128.2, 126.2, 126.2, 123.5 (q, *J* 272.5 Hz), 91.5, 63.6.

General procedure IV for acetylation reaction

2-Nitro-2-phenylethyl acetate (**4a**)

2-Nitro-2-phenylethanol (**2a**) (100 mg, 0.60 mmol, 1.0 equiv.) was dissolved in acetic anhydride (1.2 mL), and *p*-toluenesulfonic acid (1.2 mg, 0.006 mmol, 0.01 equiv.) was added. The reaction mixture was stirred at room temperature for 4 h. Upon completion, toluene was added, and the mixture was concentrated under reduced pressure to remove excess acetic anhydride by co-evaporation (3 × 10 mL). Purification by flash column chromatography on silica gel (20% EtOAc/hexanes) afforded 2-nitro-2-phenylethyl acetate (**4a**) (100 mg, 0.48 mmol, 80%) as a pale-yellow oil. Spectroscopic data for this compound is in accordance with the literature.[41] Rf = 0.51 (20% EtOAc/hexanes); ^{1}H NMR (400 MHz, $CDCl_3$) δ 7.52-7.37 (m, 5H), 5.72 (dd, *J* 10.7, 3.4 Hz, 1H), 4.95 (dd, *J* 12.4, 10.7 Hz, 1H), 4.51 (dd, *J* 12.4, 3.4 Hz, 1H), 2.09 (s, 3H); ^{13}C NMR (101 MHz, $CDCl_3$) δ 70.3, 130.7, 129.4, 127.7, 88.9, 63.9, 20.7.

2-Nitro-2-(*p*-methoxyphenyl)ethyl acetate (**4b**)

Prepared according to the general procedure IV. The product was obtained as a yellow oil (185 mg, 0.77 mmol, 77%). Rf = 0.57 (20% EtOAc/hexanes); ^{1}H NMR (400 MHz, $CDCl_3$) δ 7.39 (d, *J* 8.5 Hz, 2H), 6.92 (d, *J* 8.5 Hz, 2H), 5.67 (dd, *J* 10.7, 3.4 Hz, 1H), 4.93 (at, *J* 11.5 Hz, 1H), 4.48 (dd, *J* 12.3, 3.4 Hz, 1H), 3.82 (s, 3H), 2.09 (s, 3H); ^{13}C NMR (101 MHz, $CDCl_3$) δ 170.4, 161.4, 129.3, 122.9, 114.8, 88.5, 64.0, 55.5, 20.7; HRMS (ESI) *m/z*, calcd. for $[C_{11}H_{13}NO_5 + Na]^+$: 262.0693, found: 262.0686.

2-Nitro-2-(*p*-cyanophenyl)ethyl acetate (**4c**)

Prepared according to the general procedure IV. The product was obtained as a pale-yellow oil (87 mg, 0.37 mmol, 97%). Rf = 0.67 (40% EtOAc/hexanes); ^{1}H NMR (400 MHz, $CDCl_3$) δ 7.76 (d, *J* 8.0 Hz, 2H), 7.60 (d, *J* 8.0 Hz, 2H), 5.78 (dd, *J* 10.1, 3.6 Hz, 1H), 4.94-4.86 (m, 1H), 4.55 (dd, *J* 12.4, 3.6 Hz, 1H), 2.11 (s, 3H); ^{13}C NMR (101 MHz, $CDCl_3$) δ 170.1, 135.0, 133.1, 128.5, 117.6, 114.7, 87.9, 63.3, 20.5; HRMS (ESI) *m/z*, calcd. for $[C_{11}H_{10}N_2O_4 + K]^+$: 273.0278, found: 273.0382.

2-Nitro-2-(*p*-trifluoromethylphenyl)ethyl acetate (**4d**)

Prepared according to the general procedure IV. The product was obtained as a pale-yellow oil (50 mg, 0.18 mmol, quantitative yield) and was used without further purification due to its high instability. Rf = 0.46 (20% EtOAc/hexanes); ^{1}H NMR (400 MHz, $CDCl_3$) δ 7.71 (d, *J* 8.2 Hz, 2H), 7.61 (d, *J* 8.2 Hz, 2H), 5.80 (dd, *J* 10.5, 3.6 Hz, 1H), 4.93 (dd, *J* 12.4, 10.5 Hz, 1H), 4.55 (dd, *J* 12.4, 3.6 Hz, 1H), 2.11 (s, 3H); ^{13}C NMR (101 MHz, $CDCl_3$) δ 170.5, 134.2, 132.8 (q, *J* 33.1 Hz), 128.2, 126.4, 126.4, 123.5 (q, *J* 272.5 Hz), 88.1, 63.5, 20.5.

General procedure V for the preparation of alkyl azides

Benzyl azide (**5a**)

NaN_3 (1.1 g, 16.5 mmol, 1.1 equiv.) was dissolved in DMSO (30 mL), and benzyl bromide (2.6 g, 15.0 mmol, 1.0 equiv.) was added dropwise at room temperature under stirring. The reaction mixture was stirred for 5 h. Upon completion, water (120 mL) was added, and the mixture was extracted with diethyl ether (3 × 60 mL). The combined organic layers were washed with saturated aqueous NaCl, dried over anhydrous Na_2SO_4, filtered, and concentrated under reduced pressure to afford benzyl azide (**5a**) (1.5 g, 11.4 mmol, 84%) as a colorless oil without further purification. Spectroscopic data for this compound is in accordance with the literature.[18] Rf = 0.66 (5% EtOAc/hexanes); ^{1}H NMR (400 MHz, $CDCl_3$) δ 7.37-7.32 (m, 5H), 4.35 (s, 2H); ^{13}C NMR (101 MHz, $CDCl_3$) δ 135.4, 128.9, 128.4, 128.3, 54.9.

Dodecyl azide (**5b**)

Prepared according to the general procedure V. The product was obtained as a colorless oil (0.73 g, 3.46 mmol, 86%) without further purification. Rf = 0.71 (5% EtOAc/hexanes). Spectroscopic data for this compound is in accordance with the literature.[42] ^{1}H NMR (400 MHz, $CDCl_3$) δ 3.24 (t, *J* 7.0 Hz, 2H), 1.65-1.55 (m, 2H), 1.35-1.25 (m, 18H), 0.88 (t, *J* 6.6 Hz, 3H).

Cyclopentyl azide (**5c**)

NaN_3 (0.96 g, 14.8 mmol, 1.1 equiv.) was dissolved in DMSO (27 mL), and cyclopentyl bromide (2.0 g, 13.4 mmol, 1.0 equiv.) was added at room temperature under stirring. The reaction mixture was then heated to 80 °C and stirred overnight. After completion, water (60 mL) was added, and the mixture was extracted with diethyl ether (4 × 20 mL). The combined organic layers were washed with saturated aqueous NaCl, dried over anhydrous Na_2SO_4, filtered, and concentrated under reduced pressure to afford cyclopentyl azide (**5c**) (1.1 g, 9.9 mmol, 73%) as an orange oil without further purification. Spectroscopic data for this compound is in accordance with the literature.[43] ^{1}H NMR (400 MHz, $CDCl_3$) δ 3.98-3.89 (m, 1H), 1.89-1.59 (m, 8H); ^{13}C NMR (101 MHz, $CDCl_3$) δ 63.1, 32.2, 23.7.

General procedure VI for preparation of alkyl azides

Ethyl 2-azidoacetate (**5d**)

Ethyl 2-bromoacetate (1.66 g, 10.0 mmol, 1.0 equiv.) was dissolved in ethanol (8.0 mL), and water (4.0 mL) was added. NaN_3 (2.3 g, 20.0 mmol, 2.0 equiv.) was then added, and the reaction mixture was stirred at room temperature for 2.5 h. Upon completion, the solvent was partially removed under reduced pressure to eliminate ethanol, followed by the addition of water (20 mL). The mixture was extracted with CH_2Cl_2 (3 × 20 mL), and the combined organic layers were washed with saturated aqueous NaCl, dried over anhydrous Na_2SO_4, filtered, and concentrated under reduced pressure (caution: volatile compound) to afford ethyl 2-azidoacetate (**5d**) (0.63 g, 4.9 mmol, 49%) as a colorless oil without further purification. Spectroscopic data for this compound is in accordance with the literature.[42] Rf = 0.66 (10% EtOAc/hexanes); ^{1}H NMR (400 MHz, $CDCl_3$) δ 4.27 (q, *J* 7.1 Hz, 2H), 3.87 (s, 2H), 1.32 (t, *J* 7.1 Hz, 3H); ^{13}C NMR (101 MHz, $CDCl_3$) δ 168.3, 61.9, 50.4, 14.2.

2-Azido-1-phenylethanone (**5e**)

Prepared according to procedure VI. The product was obtained as an orange oil (0.579 g, 3.59 mmol, 72%) without further purification. Rf = 0.17 (5% EtOAc/hexanes). Spectroscopic data for this compound is in accordance with the literature.[44] ^{1}H NMR (400 MHz, $CDCl_3$) δ 7.91 (d, *J* 7.5 Hz, 2H), 7.63 (t, *J* 7.5 Hz, 1H), 7.50 (t, *J* 7.5 Hz, 2H), 4.56 (s, 2H); ^{13}C NMR (101 MHz, $CDCl_3$) δ 193.3, 134.5, 134.2, 129.1, 128.0, 55.0.

General procedure VII for preparation of arylazides

4-Azidoanisole (**5f**)

p-Methoxy-aniline (1.23 g, 10 mmol) was added in

an aqueous solution of HCl (6 M, 10 mL) at 0 ºC. After 2 min, $NaNO_2$ (15 mmol) dissolved in 25 mL of water was added dropwise to the reaction mixture. The reaction was left for 30 min under vigorous stirring. After this interval, NaN_3 (40 mmol) was dissolved in water (10 mL) and added dropwise to the reaction. The reaction was left for a further 4 h at room temperature. After the completion of the reaction, monitoring by TLC, the mixture was extracted with ethyl acetate (3 × 10 mL), the combined organic phases were washed with water and then dried over anhydrous Na_2SO_4, filtered and concentrated in vacuum to afford 4-azidoanisole (**5f**) (1.43 g, 9.6 mmol, 96% yield) as a brown oil without further purification. Spectroscopic data for this compound is in accordance with the literature.[45] ^{1}H NMR (400 MHz, $CDCl_3$) δ 6.95-6.90 (m, 2H), 6.88-6.83 (m, 2H), 3.76 (s, 3H).

Phenyl azide (**5g**)

Synthesized according to the general procedure VII. The product was obtained as light brown liquid (1.30 g, 10.9 mmol, 90%) without further purification. Spectroscopic data for this compound is in accordance with the literature.[45] ^{1}H NMR (400 MHz, $CDCl_3$) δ 7.30-7.24 (m, 2H), 7.10-7.04 (m, 1H), 6.98-6.92 (m, 2H).

General procedure VIII for preparation of 1,4-disubstituted 1,2,3-triazoles

1-Benzyl-4-phenyl-1*H*-1,2,3-triazole (**6a**)

In a 10 mL microwave vial, 2-nitro-2-phenylethyl acetate (**4a**) (50.0 mg, 0.24 mmol, 1.0 equiv.) and benzyl azide (**5a**) (35.0 mg, 0.26 mmol, 1.1 equiv.) were dissolved in anhydrous DMF (0.3 mL). PTSA (7.9 mg, 0.06 mmol, 0.25 equiv.) was then added, and the reaction mixture was subjected to microwave irradiation at 130 °C (300 W) for 50 min. After completion, ethyl acetate (10 mL) was added, and the organic phase was washed with water (2 × 5 mL) and saturated aqueous NaCl. The organic layer was dried over anhydrous Na_2SO_4, filtered, and concentrated under reduced pressure. Purification by flash column chromatography on silica gel (10-20% EtOAc/hexanes gradient) afforded 1-benzyl-4-phenyl-1*H*-1,2,3-triazole (**6a**) (40.1 mg, 0.17 mmol, 71%) as a white solid. Spectroscopic data for this compound is in accordance with the literature.[46] Rf = 0.20 (20% EtOAc/hexanes); ^{1}H NMR (400 MHz, $CDCl_3$) δ 7.82-7.77 (m, 2H), 7.66 (s, 1H), 7.43-7.35 (m, 5H), 7.34-7.28 (m, 3H), 5.58 (s, 2H); ^{13}C NMR (101 MHz, $CDCl_3$) δ 148.2, 134.6, 130.5, 129.1, 128.8, 128.2, 128.0, 125.7, 119.5, 54.2.

1-Benzyl-4-(*p*-methoxyphenyl)-1*H*-1,2,3-triazole (**6b**)

Synthesized according to general procedure VII. The product was obtained as an orange solid (35 mg, 0.13 mmol, 44%). Spectroscopic data for this compound are in accordance with the literature.[47] Rf = 0.37 (30% EtOAc/hexanes); ^{1}H NMR (400 MHz, $CDCl_3$) δ 7.71 (d, *J* 8.5 Hz, 2H), 7.57 (s, 1H), 7.41-7.25 (m, 5H), 6.92 (d, *J* 8.5 Hz, 2H), 5.54 (s, 2H), 3.81 (s, 3H); ^{13}C NMR (101 MHz, $CDCl_3$) δ 159.6, 148.1, 134.8, 129.1, 128.7, 128.0, 127.0, 123.3, 118.8, 114.2, 55.3, 54.2.

1-Benzyl-4-(*p*-cyanophenyl)-1*H*-1,2,3-triazole (**6c**)

Synthesized according to general procedure VII. The product was obtained as a yellow solid (31 mg, 0.12 mmol, 41%). Spectroscopic data for this compound are in accordance with the literature.[48] Rf = 0.34 (30% EtOAc/hexanes); ^{1}H NMR (400 MHz, $CDCl_3$) δ 7.90 (d, *J* 8.2 Hz, 2H), 7.79 (s, 1H), 7.67 (d, *J* 8.2 Hz, 2H), 7.43-7.37 (m, 3H), 7.34-7.30 (m, 2H), 5.59 (s, 2H); ^{13}C NMR (101 MHz, $CDCl_3$) δ 146.3, 134.9, 134.2, 132.6, 129.2, 129.0, 128.1, 126.0, 120.7, 118.7, 111.4, 54.4.

1-Benzyl-4-(*p*-trifluoromethylphenyl)-1*H*-1,2,3-triazole (**6d**)

Synthesized according to general procedure VII. The product was obtained as a yellow solid (10.4 mg, 0.034 mmol, 31%). Spectroscopic data for this compound are in accordance with the literature.[49] Rf = 0.26 (20% EtOAc/hexanes); ^{1}H NMR (400 MHz, $CDCl_3$) δ 7.91 (d, *J* 8.1 Hz, 2H), 7.74 (s, 1H), 7.65 (d, *J* 8.1 Hz, 2H), 7.44-7.37 (m, 3H), 7.36-7.30 (m, 2H), 5.60 (s, 2H); ^{13}C NMR (101 MHz, $CDCl_3$) δ 147.0, 134.5, 134.1, 130.1 (q, *J* 32.6 Hz), 130.0, 129.7, 129.4, 129.1, 128.3, 126.0, 124.2 (q, *J* 272.3 Hz), 120.4, 54.5; ^{19}F NMR (377 MHz, $CDCl_3$) δ −62.6.

1-Cyclopentyl-4-phenyl-1*H*-1,2,3-triazole (**6e**)

Synthesized according to general procedure VII. The product was obtained as a yellow solid (44.3 mg, 0.21 mmol, 69%). Spectroscopic data for this compound are in accordance with the literature.[50] Rf = 0.17 (20% EtOAc/hexanes); ^{1}H NMR (400 MHz, $CDCl_3$) δ 7.82 (d, *J* 7.9 Hz, 2H), 7.75 (s, 1H), 7.40 (t, *J* 7.6 Hz, 2H), 7.31 (t, *J* 7.4 Hz, 1H), 4.95 (p, *J* 6.8 Hz, 1H), 2.26 (dt, *J* 13.2, 6.8 Hz, 2H), 2.13-2.05 (m, 2H), 1.97-1.87 (m, 2H), 1.81-1.72 (m, 2H); ^{13}C NMR (101 MHz, $CDCl_3$) δ 147.6, 130.9, 128.9, 128.1, 125.7, 118.2, 62.0, 33.5, 24.2.

1-Dodecyl-4-phenyl-1*H*-1,2,3-triazole (**6f**)

Synthesized according to general procedure VII. The product was obtained as a white solid (52.0 mg, 0.17 mmol, 55%). Spectroscopic data for this compound are in accordance with the literature.[42] Rf = 0.54 (20% EtOAc/hexanes); ^{1}H NMR (400 MHz, $CDCl_3$) δ 7.83 (d, *J* 7.4 Hz,

2H), 7.74 (s, 1H), 7.41 (t, *J* 7.4 Hz, 2H), 7.32 (t, *J* 7.4 Hz, 1H), 4.37 (t, *J* 7.2 Hz, 2H), 1.98-1.88 (m, 2H), 1.35-1.20 (m, 18H), 0.87 (t, *J* 6.6 Hz, 3H); ^{13}C NMR (101 MHz, $CDCl_3$) δ 147.7, 130.8, 128.8, 128.0, 125.7, 119.4, 50.4, 31.9, 30.3, 29.6, 29.5, 29.4, 29.3, 29.0, 26.5, 22.7, 14.1.

Ethyl 2-(4-phenyl-1*H*-1,2,3-triazol-1-yl)acetate (**6g**)

Synthesized according to general procedure VII. The product was obtained as a yellow solid (50 mg, 0.22 mmol, 60%). Spectroscopic data for this compound are in accordance with the literature.[42] Rf = 0.31 (20% EtOAc/hexanes); ^{1}H NMR (400 MHz, $CDCl_3$) δ 7.92 (s, 1H), 7.83 (d, *J* 7.5 Hz, 2H), 7.42 (t, *J* 7.5 Hz, 2H), 7.33 (t, *J* 7.5 Hz, 1H), 5.18 (s, 2H), 4.26 (q, *J* 7.1 Hz, 2H), 1.29 (t, *J* 7.1 Hz, 3H); ^{13}C NMR (101 MHz, $CDCl_3$) δ 166.3, 148.2, 130.4, 128.8, 128.3, 125.8, 121.1, 62.4, 50.9, 14.1.

1,4-Diphenyl-1*H*-1,2,3-triazole (**6i**)

Synthesized according to general procedure VII. The product was obtained as a yellow solid (23.6 mg, 0.11 mmol, 45%). Spectroscopic data for this compound are in accordance with the literature.[51] Rf = 0.43 (20% EtOAc/hexanes); ^{1}H NMR (400 MHz, $CDCl_3$) δ 8.20 (s, 1H), 7.93-7.90 (m, 2H), 7.82-7.76 (m, 2H), 7.58-7.51 (m, 2H), 7.50-7.43 (m, 3H), 7.40-7.34 (m, 1H); ^{13}C NMR (101 MHz, $CDCl_3$) δ 148.4, 137.0, 130.2, 129.8, 128.9, 128.7, 128.4, 125.8, 120.5, 117.6.

1-(*p*-Methoxyphenyl)-4-phenyl-1*H*-1,2,3-triazole (**6j**)

Synthesized according to general procedure VII. The product was obtained as a brown solid (8.6 mg, 0.034 mmol, 14%). Spectroscopic data for this compound are in accordance with the literature.[52] Rf = 0.26 (20% EtOAc/hexanes); ^{1}H NMR (400 MHz, $CDCl_3$) δ 8.11 (s, 1H), 7.94-7.87 (m, 2H), 7.727.64 (m, 2H), 7.49-7.43 (m, 2H), 7.39-7.34 (m, 1H), 7.07-7.01 (m, 2H), 3.88 (s, 3H); ^{13}C NMR (101 MHz, $CDCl_3$) δ 159.8, 148.2, 130.5, 130.3, 128.9, 128.3, 125.8, 122.2, 117.8, 114.8, 55.6.

Computational methods

Density functional theory (DFT) calculations were performed with the Gaussian 16[53] program using an ultrafine grid for numerical integration. Geometry optimizations used the M06-2X/def2-TZVP[54,55] level of theory with the IEF-PCM[56] [DMF] implicit solvation model. This level of theory was selected based on previous studies that demonstrated excellent performance for cycloaddition reactions involving azides and β-nitroolefins.[18] Structures were visualized with CYLview.[57] Vibrational frequency calculations were used to confirm that stationary points were either minima or first-order saddle points on the potential energy surface and to obtain frequencies used to calculate thermochemistry values with the GoodVibes program.[58] Intrinsic reaction coordinate (IRC) calculations were carried out to ensure that the intermediates (Int) of the different pathways connected to their corresponding transition structure (TS).

Thermochemistry data and absolute energy values

Quasi-harmonic (QHA) corrections were introduced to the computed vibrational entropies with GoodVibes using a frequency cut-off value of 100.0 cm^{-1}, following the model proposed by Grimme[59] at 403.15 K (130 °C). Also, a correction for the change in standard state from the gas phase at 1 atm to a 0.75 M solution was applied. All the thermochemical data, including absolute electronic energies, Gibbs energy (G) and relative G values, zero-point energies (ZPE), and T·S are tabulated in the SI section.

Distortion/interaction analysis on the transition state

A distortion/interaction analysis was performed for the transition states (**TS-1**, **TS-2** and **TS-3**) of cycloadditions of α-nitrostyrene (**3a**) with PhN_3 (**5f**). To obtain the distorted structures, each transition state was separated into two fragments (distorted 1,3-dipoles and dipolarophiles), followed by single-point energy calculations at the M06-2X/def2-TZVP level of theory. Distortion energies ($\Delta E_d^{\ddagger}$) of α-nitrostyrene and azides were obtained by the energy differences between the distorted structures and ground-state structures. The difference between the activation energy ($\Delta E^{\ddagger}$) and the total distortion energy ($\Delta E_{d,total}^{\ddagger} = \Delta E_{d,azide}^{\ddagger} + \Delta E_{d,\alpha\text{-nitrostyrene}}^{\ddagger}$) represents the interaction energy ($\Delta E_i^{\ddagger}$).

Supplementary Information

Supplementary information (initial investigation details; ^{1}H NMR and ^{13}C NMR spectra of compounds; energies and cartesian coordinates of all calculated structures; IRC plots) are available free of charge at http://jbcs.sbq.org.br as PDF file.

Data Availability Statement

The data supporting this article is available in the text.

Acknowledgments

We are grateful to CNPq, CAPES, and FAPESP (2017/01754-0, 2021/12394-0) for financial support.

Author Contributions

M.Y.K.: synthesis, investigation, theoretical calculations; M. A. B. F. writing, conceptualization, supervision, resources, founding acquisition.

References

1. Wamhoff, H. In *Comprehensive Heterocyclic Chemistry*, vol. 5, 1st ed.; Katritzky, A. R.; Rees, C. W., eds.; Pergamon, 1984, p. 669. [Crossref]
2. Agalave, S. G.; Maujan, S. R.; Pore, V. S.; *Chem. Asian J.* **2011**, *6*, 2696. [Crossref]
3. Hein, J. E.; Fokin, V. V.; *Chem. Soc. Rev.* **2010**, *39*, 1302. [Crossref]
4. Moses, J. E.; Moorhouse, A. D.; *Chem. Soc. Rev.* **2007**, *36*, 1249. [Crossref]
5. Schulze, B.; Schubert, U. S.; *Chem. Soc. Rev.* **2014**, *43*, 2522. [Crossref]
6. Liang, L.; Astruc, D.; *Coord. Chem. Rev.* **2011**, *255*, 2933. [Crossref]
7. Huisgen, R.; *Angew. Chem., Int. Ed.* **1963**, *2*, 565. [Crossref]
8. Huisgen, R.; *Angew. Chem., Int. Ed.* **1963**, *2*, 633. [Crossref]
9. Kolb, H. C.; Finn, M. G.; Sharpless, K. B.; *Angew. Chem., Int. Ed.* **2001**, *40*, 2004. [Crossref]
10. Rostovtsev, V. V.; Green, L. G.; Fokin, V. V.; Sharpless, K. B.; *Angew. Chem., Int. Ed.* **2002**, *41*, 2596. [Crossref]
11. Tornøe, C. W.; Christensen, C.; Meldal, M.; *J. Org. Chem.* **2002**, *67*, 3057. [Crossref]
12. Meldal, M.; Tornøe, C. W.; *Chem. Rev.* **2008**, *108*, 2952. [Crossref]
13. Zhang, L.; Chen, X.; Xue, P.; Sun, H. H. Y.; Williams, I. D.; Sharpless, K. B.; Fokin, V. V.; Jia, G.; *J. Am. Chem. Soc.* **2005**, *127*, 15998. [Crossref]
14. Baskin, J. M.; Prescher, J. A.; Laughlin, S. T.; Agard, N. J.; Chang, P. V.; Miller, I. A.; Lo, A.; Codelli, J. A.; Bertozzi, C. R.; *Proc. Natl. Acad. Sci. USA* **2007**, *104*, 16793. [Crossref]
15. Jewett, J. C.; Bertozzi, C. R.; *Chem. Soc. Rev.* **2010**, *39*, 1272. [Crossref]
16. Chiavegatti Neto, A.; Soares, K. C.; Santos, M. S.; Aímola, T. J.; Ferreira, A. G.; Jardim, G. A. M.; Tormena, C. F.; Paixão, M. W.; Ferreira, M. A. B.; *Org. Biomol. Chem.* **2022**, *20*, 6019. [Crossref]
17. Revathi, S.; Meena, M.; Ghatak, T.; *Results Chem.* **2026**, *19*, 102949. [Crossref]
18. Kawamura, M. Y.; Alegre-Requena, J. V.; Barbosa, T. M.; Tormena, C. F.; Paton, R. S.; Ferreira, M. A. B.; *Chem. Eur. J.* **2022**, *28*, e202202294 [Crossref]
19. Ess, D. H.; Houk, K. N.; *J. Am. Chem. Soc.* **2007**, *129*, 10646. [Crossref]
20. Lopez, S. A.; Munk, M. E.; Houk, K. N.; *J. Org. Chem.* **2013**, *78*, 1576. [Crossref]
21. Tajabadi, J.; Bakavoli, M.; Gholizadeh, M.; Eshghi, H.; *Org. Biomol. Chem.* **2016**, *14*, 7324. [Crossref]
22. Sahu, D.; Dey, S.; Pathak, T.; Ganguly, B.; *Org. Lett.* **2014**, *16*, 2100. [Crossref]
23. Zefirov, N. S.; Chapovskaya, N. K.; Kolesnikov, V. V.; *J. Chem. Soc. D* **1971**, 1001. [Crossref]
24. Amantini, D.; Fringuelli, F.; Piermatti, O.; Pizzo, F.; Zunino, E.; Vaccaro, L.; *J. Org. Chem.* **2005**, *70*, 6526. [Crossref]
25. D'Ambrosio, G.; Fringuelli, F.; Pizzo, F.; Vaccaro, L.; *Green Chem.* **2005**, *7*, 874. [Crossref]
26. Habib, P. M.; Rama Raju, B.; Kavala, V.; Kuo, C.-W.; Yao, C.-F.; *Tetrahedron* **2009**, *65*, 5799. [Crossref]
27. Wang, T.; Hu, X.-C.; Huang, X.-J.; Li, X.-S.; Xie, J.-W.; *J. Braz. Chem. Soc.* **2012**, *23*, 1119. [Crossref]
28. Quan, X.-J.; Ren, Z.-H.; Wang, Y.-Y.; Guan, Z.-H.; *Org. Lett.* **2014**, *16*, 5728. [Crossref]
29. Wang, Y.-C.; Xie, Y.-Y.; Qu, H.-E.; Wang, H.-S.; Pan, Y.-M.; Huang, F.-P.; *J. Org. Chem.* **2014**, *79*, 4463. [Crossref]
30. Thomas, J.; John, J.; Parekh, N.; Dehaen, W.; *Angew. Chem., Int. Ed.* **2014**, *53*, 10155. [Crossref]
31. Chen, Y.; Nie, G.; Zhang, Q.; Ma, S.; Li, H.; Hu, Q.; *Org. Lett.* **2015**, *17*, 1118. [Crossref]
32. Chen, Z.; Zhang, Y.; Nie, J.; Ma, J.-A.; *Org. Lett.* **2018**, *20*, 2120. [Crossref]
33. Lugiņina, J.; Rjabovs, V.; Belyakov, S.; Turks, M.; *Tetrahedron Lett.* **2013**, *54*, 5328. [Crossref]
34. Wang, T.; Shao, A.; Feng, H.; Yang, S.; Gao, M.; Tian, J.; Lei, A.; *Tetrahedron* **2015**, *71*, 4473. [Crossref]
35. Greger, J. G.; Yoon-Miller, S. J. P.; Bechtold, N. R.; Flewelling, S. A.; MacDonald, J. P.; Downey, C. R.; Cohen, E. A.; Pelkey, E. T.; *J. Org. Chem.* **2011**, *76*, 8203. [Crossref]
36. Zhu, C.; Han, M.-Y.; Liang, X.-X.; Guan, B.; Li, P.; Wang, L.; *Org. Lett.* **2021**, *23*, 54. [Crossref]
37. Miyashita, M.; Yanami, T.; Yoshikoshi, A.; *Org. Synth.* **1981**, *60*, 101. [Crossref]
38. Lešetický, L.; Fidler, V.; Procházka, M.; *Collect. Czechoslov. Chem. Commun.* **1973**, *38*, 459. [Crossref]
39. Walvoord, R. R.; Berritt, S.; Kozlowski, M. C.; *Org. Lett.* **2012**, *14*, 4086. [Crossref]
40. Alaime, T.; Delots, A.; Pasquinet, E.; Suzenet, F.; Guillaumet, G.; *Tetrahedron* **2016**, *72*, 1337. [Crossref]
41. N. V. G., M.; Dyapa, R.; Pansare, S. V.; *Org. Lett.* **2015**, *17*, 5312. [Crossref]
42. Alonso, F.; Moglie, Y.; Radivoy, G.; Yus, M.; *Eur. J. Org. Chem.* **2010**, *2010*, 5913. [Crossref]
43. Alvarez, S. G.; Alvarez, M. T.; *Synthesis* **1997**, *1997*, 413. [Crossref]
44. Kholod, I.; Vallat, O.; Buciumas, A.; Neels, A.; Neier, R.; *Eur. J. Org. Chem.* **2014**, *2014*, 7865. [Crossref]

45. Sebest, F.; Casarrubios, L.; Rzepa, H. S.; White, A. J. P.; Díez-González, S.; *Green Chem.* **2018**, *20*, 4023. [Crossref]
46. Shin, J.-A.; Lim, Y.-G.; Lee, K.-H.; *J. Org. Chem.* **2012**, *77*, 4117. [Crossref]
47. Topchiy, M. A.; Ageshina, A. A.; Gribanov, P. S.; Masoud, S. M.; Akmalov, T. R.; Nefedov, S. E.; Osipov, S. N.; Nechaev, M. S.; Asachenko, A. F.; *Eur. J. Org. Chem.* **2019**, *2019*, 1016. [Crossref]
48. Grob, J. E.; Nunez, J.; Dechantsreiter, M. A.; Hamann, L. G.; *J. Org. Chem.* **2011**, *76*, 10241. [Crossref]
49. Karan, C. K.; Sau, M. C.; Bhattacharjee, M.; *Chem. Comm.* **2017**, *53*, 1526. [Crossref]
50. Chen, Z.; Yan, Q.; Yi, H.; Liu, Z.; Lei, A.; Zhang, Y.; *Chem. Eur. J.* **2014**, *20*, 13692. [Crossref]
51. Loukopoulos, E.; Abdul-Sada, A.; Csire, G.; Kállay, C.; Brookfield, A.; Tizzard, G. J.; Coles, S. J.; Lykakis, I. N.; Kostakis, G. E.; *Dalton Trans.* **2018**, *47*, 10491. [Crossref]
52. Kaboudin, B.; Mostafalu, R.; Yokomatsu, T.; *Green Chem.* **2013**, *15*, 2266. [Crossref]
53. Frisch, M. J.; Trucks, G. W.; Schlegel, H. B.; Scuseria, G. E.; Robb, M. A.; Cheeseman, J. R.; Scalmani, G.; Barone, V.; Petersson, G. A.; Nakatsuji, H.; Li, X.; Caricato, M.; Marenich, A. V; Bloino, J.; Janesko, B. G.; Gomperts, R.; Mennucci, B.; Hratchian, H. P.; Ortiz, J. V; Izmaylov, A. F.; Sonnenberg, J. L.; Williams-Young, D.; Ding, F.; Lipparini, F.; Egidi, F.; Goings, J.; Peng, B.; Petrone, A.; Henderson, T.; Ranasinghe, D.; Zakrzewski, V. G.; Gao, J.; Rega, N.; Zheng, G.; Liang, W.; Hada, M.; Ehara, M.; Toyota, K.; Fukuda, R.; Hasegawa, J.; Ishida, M.; Nakajima, T.; Honda, Y.; Kitao, O.; Nakai, H.; Vreven, T.; Throssell, K.; Montgomery Jr., J. A.; Peralta, J. E.; Ogliaro, F.; Bearpark, M. J.; Heyd, J. J.; Brothers, E. N.; Kudin, K. N.; Staroverov, V. N.; Keith, T. A.; Kobayashi, R.; Normand, J.; Raghavachari, K.; Rendell, A. P.; Burant, J. C.; Iyengar, S. S.; Tomasi, J.; Cossi, M.; Millam, J. M.; Klene, M.; Adamo, C.; Cammi, R.; Ochterski, J. W.; Martin, R. L.; Morokuma, K.; Farkas, O.; Foresman, J. B.; Fox, D. J.; *Gaussian 16, Revision C.01*; Gaussian, Inc., Wallingford CT, 2016.
54. Zhao, Y.; Truhlar, D. G.; *Theor. Chem. Acc.* **2008**, *120*, 215. [Crossref]
55. Weigend, F.; Ahlrichs, R.; *Phys. Chem. Chem. Phys.* **2005**, *7*, 3297. [Crossref]
56. Tomasi, J.; Mennucci, B.; Cancès, E.; *J. Mol. Struct.* **1999**, *464*, 211. [Crossref]
57. Legault, C. Y.; *CYLView*, 1.0b; Université de Sherbrooke, Canada, 2009. [Link] accessed in May 2026
58. Luchini, G.; Alegre-Requena, J. V.; Funes-Ardoiz, I.; Paton, R. S.; *F1000Res.* **2020**, *9*, 291. [Crossref]
59. Grimme, S.; *Chem. Eur. J.* **2012**, *18*, 9955. [Crossref]

Submitted: April 4, 2026
Accepted Article online: May 4, 2026
Final version online: May 21, 2026